Received: 17 February 2020 | Revised: 4 April 2020 | Accepted: 4 April 2020

DOI: 10.1002/ansa.202000010

ANALYTICAL SCIENCE ADVANCES

WILEY

FULL ARTICLE

Development of *Aloe vera*-titanium oxide-based ultrasensitive sensor for the quantification of quercetin

Antony Nitin Raja | **Annu Pandey** | **Rajeev Jain**

School of Studies in Chemistry, Jiwaji University, Gwalior, India

Correspondence
Antony Nitin Raja, School of Studies in Chemistry, Jiwaji University, Gwalior 474011, India.
Email: 12nitinraja@gmail.com

Abstract

In the present work, a novel sensor developed for the quantification of quercetin (QRC) is being reported. Due to synergistic effects of *Aloe vera* and titanium oxide, voltammetric performance of the developed sensor (ALV-TiO_2/glassy carbon electrode) was greatly enhanced. The fabricated sensor was characterized by scanning electron microscopy, X-ray diffraction, energy dispersive X-ray, and electrochemical impedance spectroscopy. The sensor was applied to study electrochemical behavior of QRC using square wave voltammetry. Under optimal condition, the developed sensor exhibited a linear response in the range of 3.3×10^{-7} to 2.31×10^{-6} μM with a detection limit of 0.8 nM. The analytical utility of the proposed sensor was justified by applying it for the analysis of QRC in real samples.

KEYWORDS

Aloe vera, quercetin, scanning electron microscopy, titanium oxide, voltammetric sensor

1 | INTRODUCTION

Quercetin (QRC), flavonoid, is abundantly found in fruits, vegetables, and other herbs. Over 130 preparations of drug have been registered worldwide, different types of flavonoids.[1-2] Apart from antioxidant activity, flavonoids may also show pro-oxidant activity under specific conditions. Many studies have shown that QRC may play a vital role in cancer prevention and in cardiovascular status improvement, and it also has real benefits in inflammatory and respiratory diseases.[3-7] Determination of QRC with high sensitivity is of vital importance from the therapeutics' point of view.[8] Onions ranked highest in QRC content in a study of 28 vegetables and nine fruits. The amount of QRC in onions varies depending on bulb color and type, being distributed mostly in the outer skins and rings.[9-10] Several techniques, namely, high-performance liquid chromatography[11-14] spectrophotometry,[15-16] gas chromatography with mass spectrometry,[17-18] and capillary electrophoresis, have been applied for the quantification of QRC.[19] But these techniques suffer from demerits such as requirement of complex and time-consuming pretreatments and expensive experimental equipment. Compared with these methods, electrochemical techniques have advantages of high sensitivity, accuracy, simplicity, low costs, and the possibility of miniaturization. Therefore, simpler electrochemical approaches have been developed for QRC determination in a wide range of matrices.[20-26]

In recent years, metal nanoparticles have been the focus of current research in designing and constructing of chemo/biosensors due to their large surface to volume ratio, strong adsorption ability, good electrical properties, high surface reaction activity, small particle size, and good surface properties.[27-29] Titanium oxide has widely been used by researchers for the fabrication of voltammetric sensors for determination of different analyte.[30-37] *Aloe vera* is a perennial plant of the lily (*Liliaceae*) or *Aloeaceae* family. *Aloe vera* contains calcium, chromium, copper, selenium, magnesium, manganese, potassium, sodium, zinc, niobium, and so forth.

In the present work, a novel sensor based on *Aloe vera*-titanium oxide nanocomposite has been developed for quantification of QRC. To the best of our knowledge, this is the first sensor for the analysis of QRC. The developed sensor was also applied for the determination of QRC in real samples.

2 | EXPERIMENTAL SECTION

2.1 | Chemicals and reagent

QRC standard was procured from TCI Chemicals and used as received. AR (Analytical Reagent) grade KCl as supporting electrolyte and ethanol as solvent were used in the study. NaOH, boric acid, acetic acid, and phosphoric acid were used for the preparation of BR buffer in the present investigation. Chemicals used were of AR grade and used without any further purification. Milli Q water was used throughout the study.

2.2 | Apparatus and measurements

Electrochemical measurements were performed using a μ AUTOLAB TYPE III (Eco-Chemie B.V., Utrecht, The Netherlands) potentiostat-galvanostat with 757 VA computrace software. *Aloe vera*-titanium oxide/glassy carbon electrode (GCE) as the working electrode, Ag/AgCl as reference electrode, and platinum wire as auxiliary electrode were used. Prior to analysis, all the solutions examined by electrochemical techniques were purged for 10 min with purified nitrogen gas.

2.3 | Preparation of *Aloe vera*-titanium oxide nanocomposite

To obtain *Aloe vera*-titanium oxide nanocomposite, 1.0 g of anatase titanium oxide nanopowder was suspended in 10 mL water. This solution was well stirred on a hot plate at 45°C for 20 min followed by addition of 2.0 g of *Aloe vera* extract gel and further stirred for 15-20 min. After obtaining a uniform mixture, it was kept at 70°C for drying in hot air oven for 3-4 h to obtain the nanocomposite.

2.4 | Fabrication of ALV-TiO_2/GC sensor

Prior to electrode modification, the GCE surface was polished with alumina powder of different particle size on microcloth pads followed by rinsing thoroughly with Milli Q water until a mirror like finish was obtained. Then, the GCE was sonicated in ethanol and distilled water for 5 min to remove adsorbed alumina particles on the electrode surface. *Aloe vera*-titanium oxide was dispersed in DMF (Dimethyl Formamide) and sonicated for 2 h to get a suspension of 1 mg/mL. In total, 4 μL of the above suspension was casted by microsyringe onto the surface of freshly polished GCE and dried at room temperature for 30-40 min to obtain the ALV-TiO_2/GC sensor. After each modification, sensor was regenerated by polishing with alumina and thoroughly washing the electrode with Milli Q water.

3 | RESULT AND DISCUSSION

3.1 | Characterization of the developed sensor

3.1.1 | Effective surface area

The effective surface area of GCE, TiO_2/GC, and ALV-TiO_2/GC sensors was calculated using Randles Savcik equation. The study was carried out using 1.0 mM potassium ferricyanide prepared in 0.1 M potassium chloride (KCl) solution (Figure 1). According to Randles-Savcik equation,

$$I = (2.69 \times 10^5)\, A \cdot C \cdot D^{1/2} n^{3/2} \mu^{1/2}, \quad (1)$$

where I represents the peak current, A represents the effective surface area of the electrode, C represents the concentration of potassium ferrocyanide solution in mole/cm^3, D represents the diffusion coefficient in cm^2/s (and its value is 7.6×10^{-6}), and μ represents scan rate in V/s.

By substituting the values in the above equation, the electroactive surface area of various sensors was calculated. The obtained effective surface area for *Aloe vera*-titanium oxide/GCE was found to be 0.063, for titanium oxide-GCE, and 0.044 for bare GCE 0.032cm^2. A higher surface area

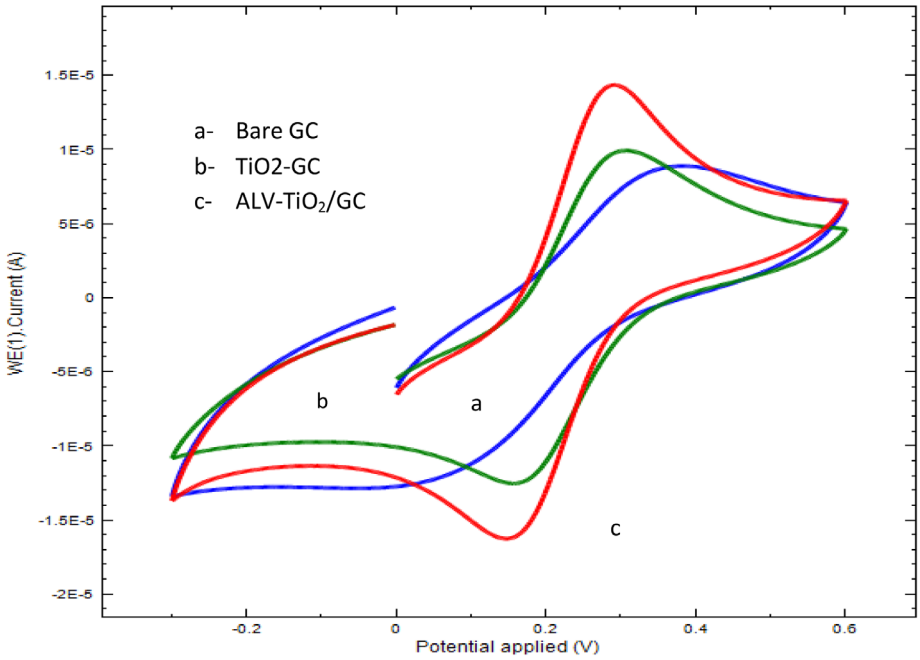

FIGURE 1 Cyclic voltammograms of 1.0 mM $K_3Fe(CN)_6$ at bare glassy carbon electrode (GCE) (a), TiO2-GCE (b), and ALV-TiO_2/GCE (c)

of ALV-TiO_2/GC sensor indicates the superiority of the modified electrode for the oxidation of QRC. The surface area observed for ALV-TiO_2/GC nanocomposite sensor was found to be larger than TiO_2/GC and bare GCE (0.035 cm^2) suggesting an enhanced voltammetric performance toward the oxidation of QRC. It can be further evident from Figure 1 indicating the voltammograms recorded at the scan rate of 100 mV/s for every sensor in which the modified sensor electrode, that is, ALV-TiO2/GC, demonstrated the highest peak current as compared to TiO_2/GC and bare GCE. Hence, the improved electroactive behavior of ALV-TiO_2 nanocomposite sensor was believed to raise the electrocatalytic oxidation of QRC.

3.1.2 | Electrochemical impedance spectroscopy

Electrochemical impedance spectroscopy was employed as experimental method to characterize the electron transfer properties of bare and modified electrodes. Nyquist plots of bare GCE and ALV-TiO2/GCE were recorded in the presence of 3.0 mM $KM_3[Fe(CN)_6]$ solution in 0.1 M KCl. Nyquist plot of impedance spectra exhibits semicircle portion at higher frequencies, which corresponds to electron transfer limited process, and linear portion at lower frequencies corresponds to diffusion process. Obtained results clearly demonstrate that lower charge transfer ratio for ALV-TiO_2/GCE is responsible for its excellent electrical conductivity, which can be attributed to availability of large surface area for electrode reaction (Figure 2). By fitting the data using appropriate equivalent circuit, values of Rct (Charge transfer resistance) were found to be 34.8 kΩ (for bare GCE), 9.87 kΩ (for TiO_2/GCE), and 5.10 kΩ (for ALV-TiO_2/GCE).

3.1.3 | X-ray diffraction study

X-ray diffraction (XRD) analysis of TiO_2 (Figure 3A) shows typical peaks at 2θ equal to 27.34°, 39.64°, 50.1°, 58.12°, 70.58°, 78.86°, and 82.62° corresponding to (435), (310), (212), (152), (197), (162), and (135) planes TiO_2 nanocomposite.

The XRD analysis of the *Aloe vera*-TiO_2 nanocomposite (Figure 3B) shows the typical peaks at 2θ equal to 12.34°, 22.64°, 35.1°, 48.12°, 60.3° and 82.62° corresponding to (535), (340), (202), (150), (180), and (162) planes *Aloe vera*-TiO_2 nanocomposite, respectively.

3.1.4 | Energy dispersive X-ray

Figure 4A represents energy dispersive X-ray (EDX) spectrum of TiO_2 nanocomposite. Spectrum clearly represents peak corresponding to titanium, carbon, and oxygen confirming the formation of TiO_2 film. Figure 4B represents EDX spectrum of *Aloe vera*-TiO_2 nanocomposite. Spectrum clearly represents peak corresponding to iron, nickel, niobium, and oxygen illustrating the formation of *Aloe vera*/TiO_2 nanocomposite film.

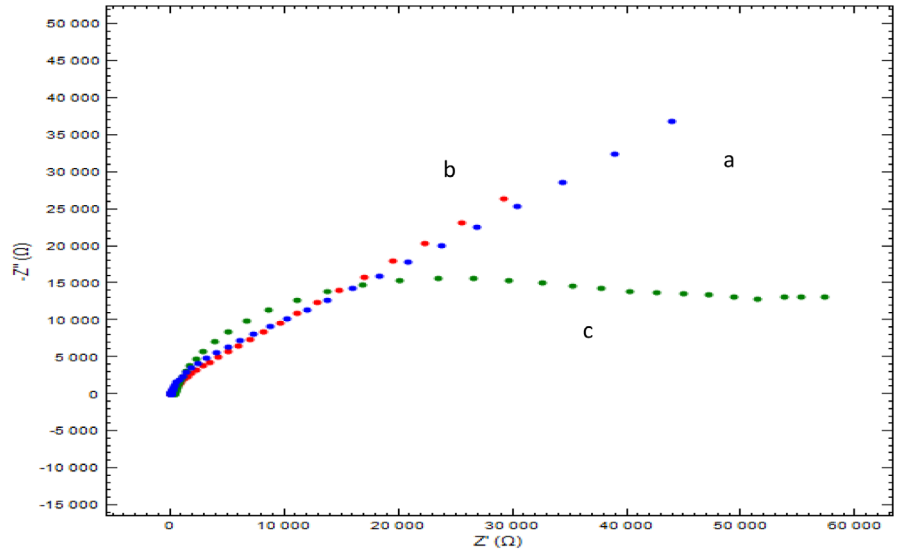

FIGURE 2 Nyquist plot of bare glassy carbon electrode (GCE) (a), TiO_2/GCE (b), and ALV-TiO_2/GCE (c)

3.1.5 | Scanning electron microscopy

Figure 5A depicts the scanning electron microscopy image of TiO_2 nanoparticles. These nanoparticles are spherically shaped and appear as a huge mass of granular particles, whereas ALV-TiO_2 (Figure 5B) has rough and uneven surface revealing a large surface area and confirming the formation of *Aloe vera*-titanium oxide nanocomposite.

3.2 | Optimization of experimental parameters

3.2.1 | Effect of pH

Effect of pH was studied with BR and phosphate buffers. Deviation in the peak potentials was observed on changing the pH value (Figure 6A) as well as current. On plotting a graph between pH and current, it was observed that QRC exhibited maximum response at pH 3.0 in BR buffer (Figure 8B). From the figure, it is clear that after pH 3.0, the anodic current decreases gradually. Shifting of peak potential with pH indicates the involvement of protons in the electrode process. A linear relationship was observed between peak potential (Ep) of QRC and pH, which can be expressed by Equation (1):

$$Ep/V\,(Ag/AgCl) = -0.075 + 0.5648R^2 = 0.992. \quad (2)$$

3.2.2 | Casting volume

The effect of loading of the *Aloe vera*-titanium oxide suspension on the surface of GC sensor was also studied. It was observed that with the increase in the loading volume, the peak current also increased. From Figure 7, it is clear that the peak current increased up to 4 μL and after that peak current decreases gradually. The decrease in anodic peak current may be attributed to the presence of a thick layer of modifier, due to which the process of electron transfer became slow. As highest peak response was obtained at 4 μL, therefore this loading volume was selected for further experimental studies.

3.2.3 | Effect of solvent system

The effect of different solvents (methanol, ethanol, DMF, TRX (Triton X-100), SLS (Sodium Lauryl Sulfate), and tween 20) on QRC oxidation was studied by square wave voltammetry. Highest anodic peak current was obtained in ethanol (Figure 8). Therefore, ethanol was employed as the solvent during all experiment.

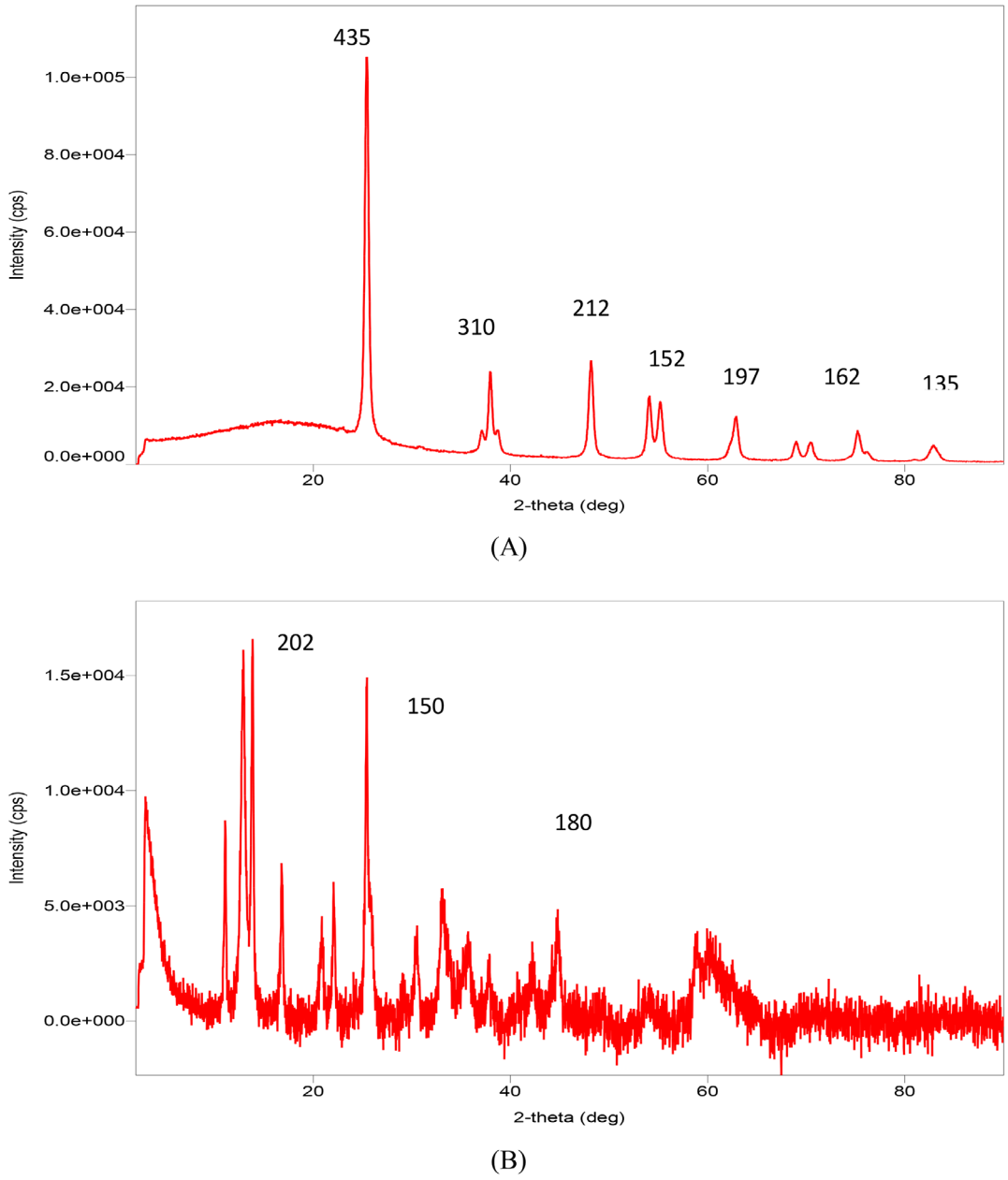

FIGURE 3 A, XRD pattern of Titanium oxide. B, XRD pattern of *Aloe vera*-titanium oxide

3.2.4 | Effect of scan rate

Cyclic voltammetry was used to study the reaction kinetics of QRC at ALV-TiO_2/GC sensor. Cyclic voltammograms of QRC (0.1 mM) were recorded at different scan rates. A total of 1.0 M KCl was used as supporting electrolyte. At fixed concentration of QRC, the scan rates were varied from 10 to 100 mV/s. On increasing scan rate, peak current also increases. A graph was plotted between the peak current (I) and the square root of the scan rate. A linear relationship was observed (Figure 9A). The regression equation can be expressed as

$$I\,(\mu A) = 2.172\,(\mathrm{mV}/s) + 2.778R^2 = 0.998. \tag{2}$$

A calibration graph was plotted between log of current and log of scan rate (Figure 9B). As the value of slope is found to be 0.71, which is close to one, the process was assumed as diffusion controlled:

$$\mathrm{Log}\ I\ (\mu A) = 0.71\,(\mathrm{mV}/s) + 0.047R^2 = 0.954. \tag{3}$$

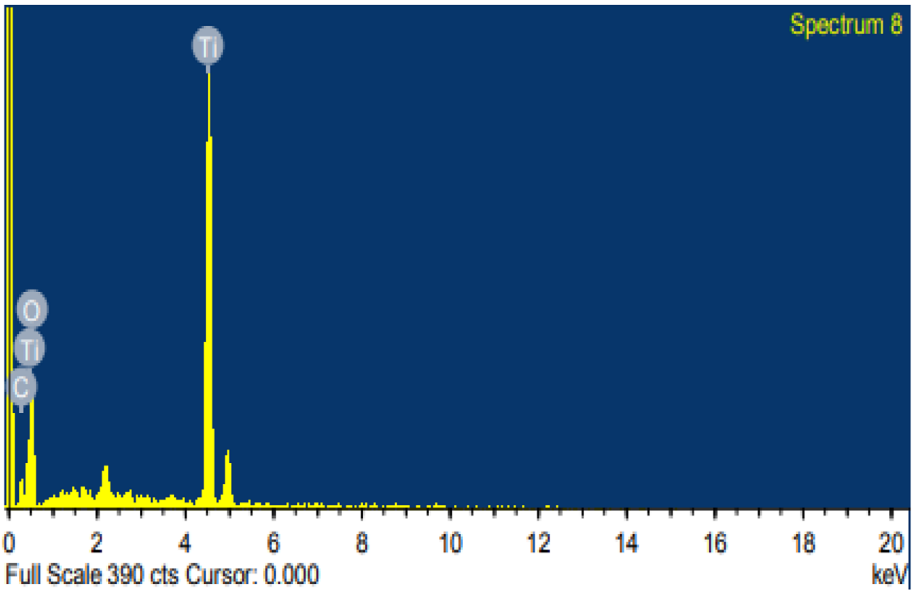

(A)

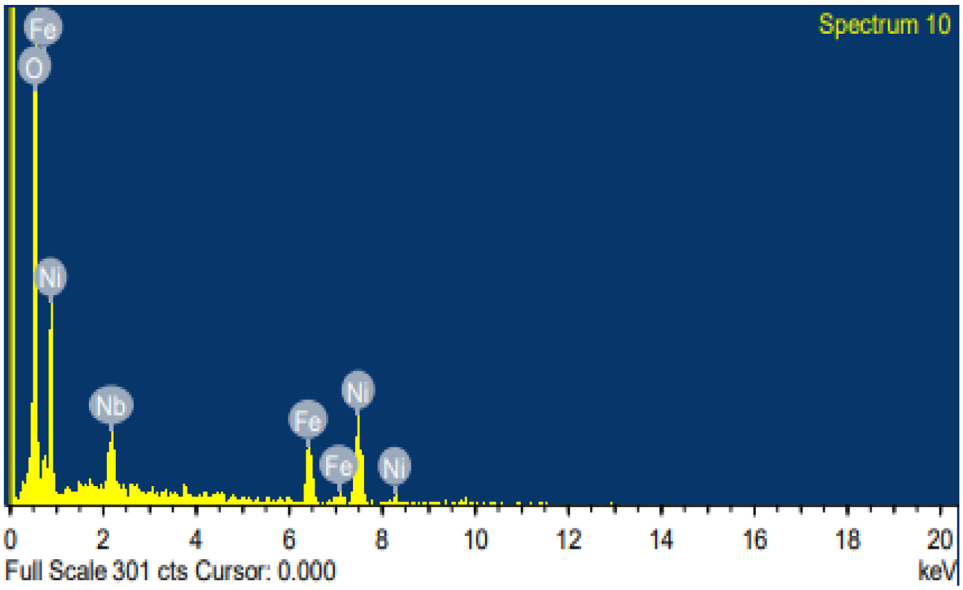

(B)

FIGURE 4 A, Energy dispersive X-ray (EDX) spectrum of titanium oxide. B, EDX spectrum of *Aloe vera*-titanium oxide

The linear relation between Ep and natural logarithm of scan rate (ln ν) (Figure 9C) followed the equation

$$Ep = E^0 + (RT/\alpha nF)\ln(RTk/\alpha nF) + (RT/\alpha nF)\ln \nu. \quad (4)$$

The slope of equation no would be equal to

$$Ep = RT/\alpha nF, \quad (5)$$

where E^0 denotes the formal potential, α denotes the transfer coefficient, k denotes the standard rate of reaction, n denotes the number of electron involved in the electrode process, and υ denotes the scan rate.

From Equation (5),

$$n = 2.4.$$

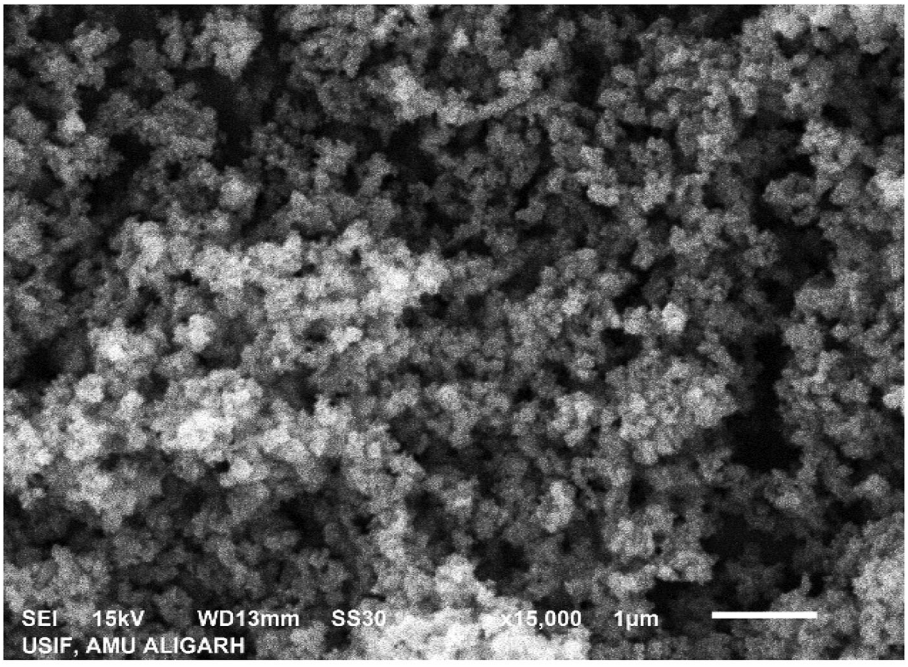

(A)

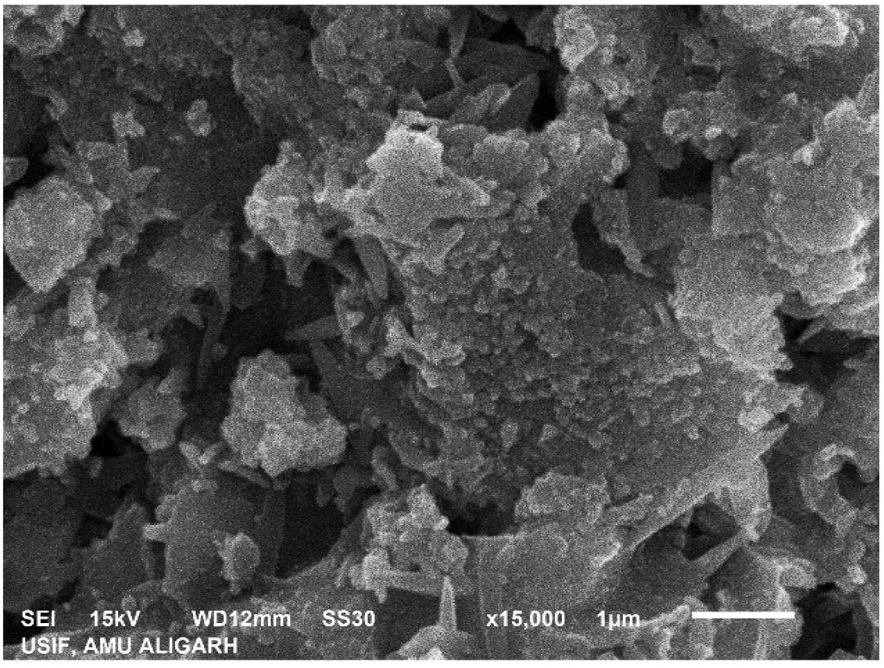

(B)

FIGURE 5 A, Scanning electron micrograph of titanium oxide. B, Scanning electron microscopy image of ALV-TiO_2

Thus, the number of electrons involved in the oxidation process was calculated to be 2.4, that is, 2 (Scheme 1).

3.3 | Electrocatalytic behavior of ALV-TiO_2/GC sensor toward the determination of QRC

The electrochemical response of QRC was investigated by square wave voltammetry and voltammograms were recorded in BR buffer of pH 3.0. QRC exhibits a well-defined oxidation peak at ALV-TiO_2/GC sensor. For comparison, peak response was also recorded at bare GCE and TiO_2/GCE. It is clear from the Figure 10 that the fabricated sensor exhibited an improved electrocatalytic response toward the detection of QRC at TiO_2/GCE. The improved peak response at the fabricated sensor demonstrates the superiority of the developed sensor.

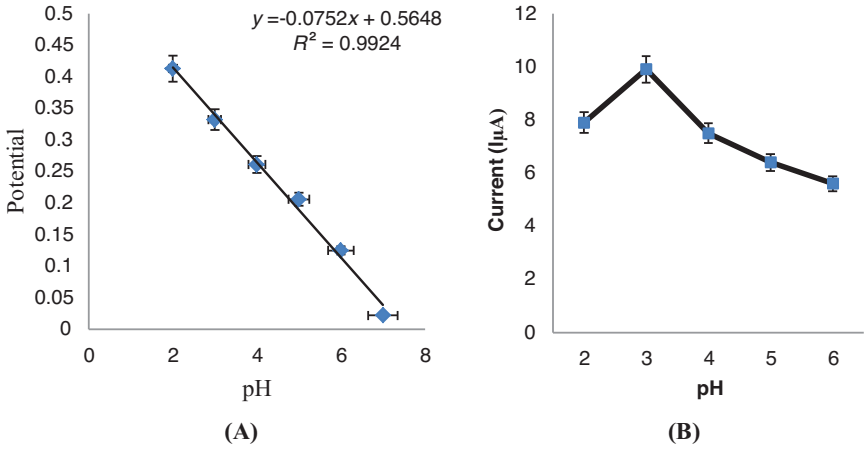

FIGURE 6 A, Plot of pH versus potential. B, Plot of pH versus current

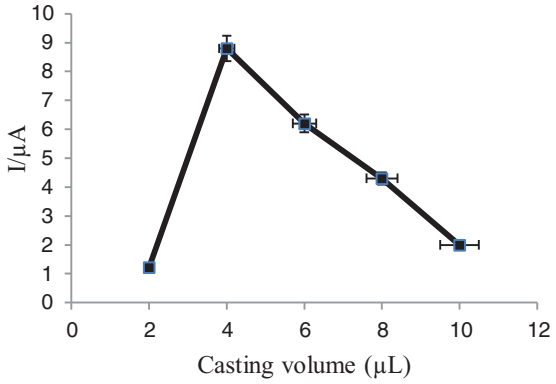

FIGURE 7 Effect of loading volume on current

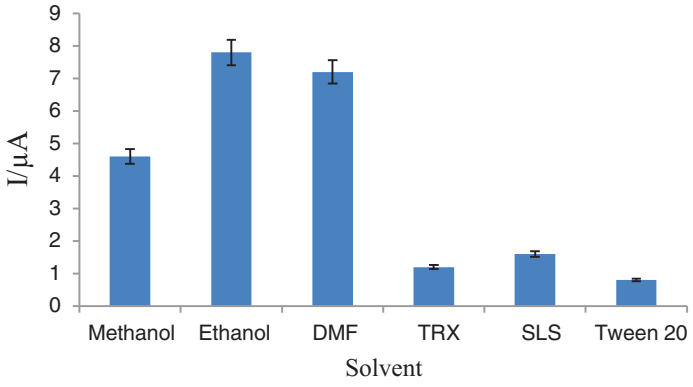

FIGURE 8 Peak current of QRC in different solvents

4 | VALIDATION OF THE PROPOSED METHOD

4.1 | Linearity

The square wave voltammograms were recorded with increasing concentration of QRC. The anodic peak current increased linearly with increase in concentration (Figure 11). Each point of the calibration graph corresponds to the mean value obtained from three independent measurements. Linear calibration curve was obtained for QRC in the range of 0.01-0.07 μg/mL in BR (Britton Robinson) buffer pH 3.0.

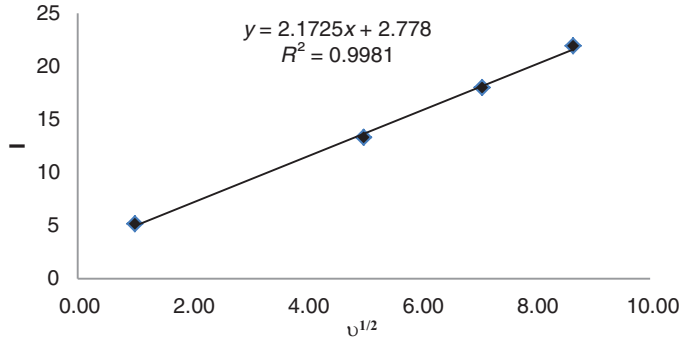

(A)

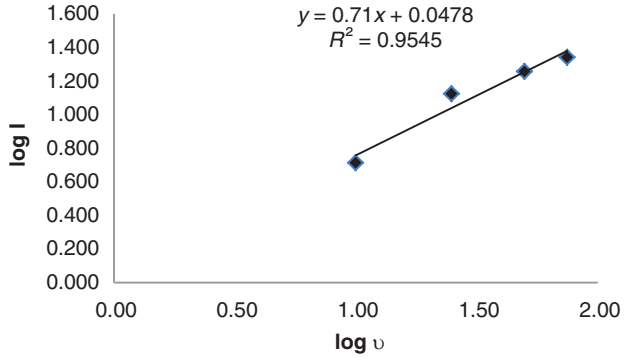

(B)

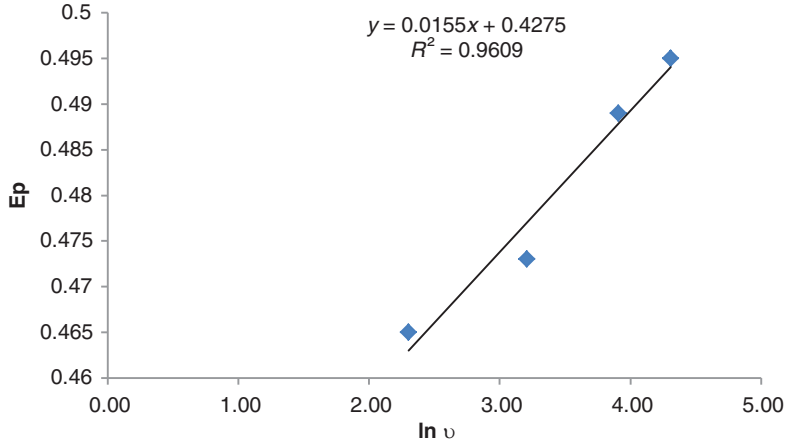

(C)

FIGURE 9 Plot of (A) $\nu^{1/2}$ versus current (*I*), (B) log ν versus log I, and (C) ln ν versus Ep

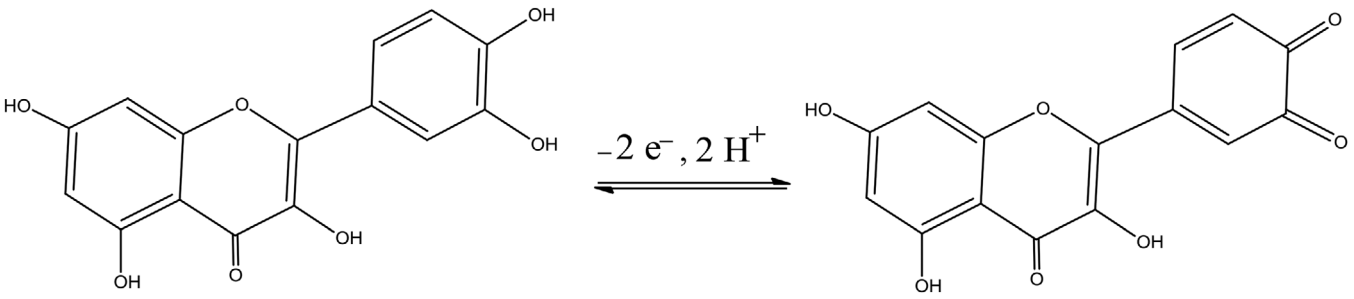

SCHEME 1 Reaction mechanism of QRC

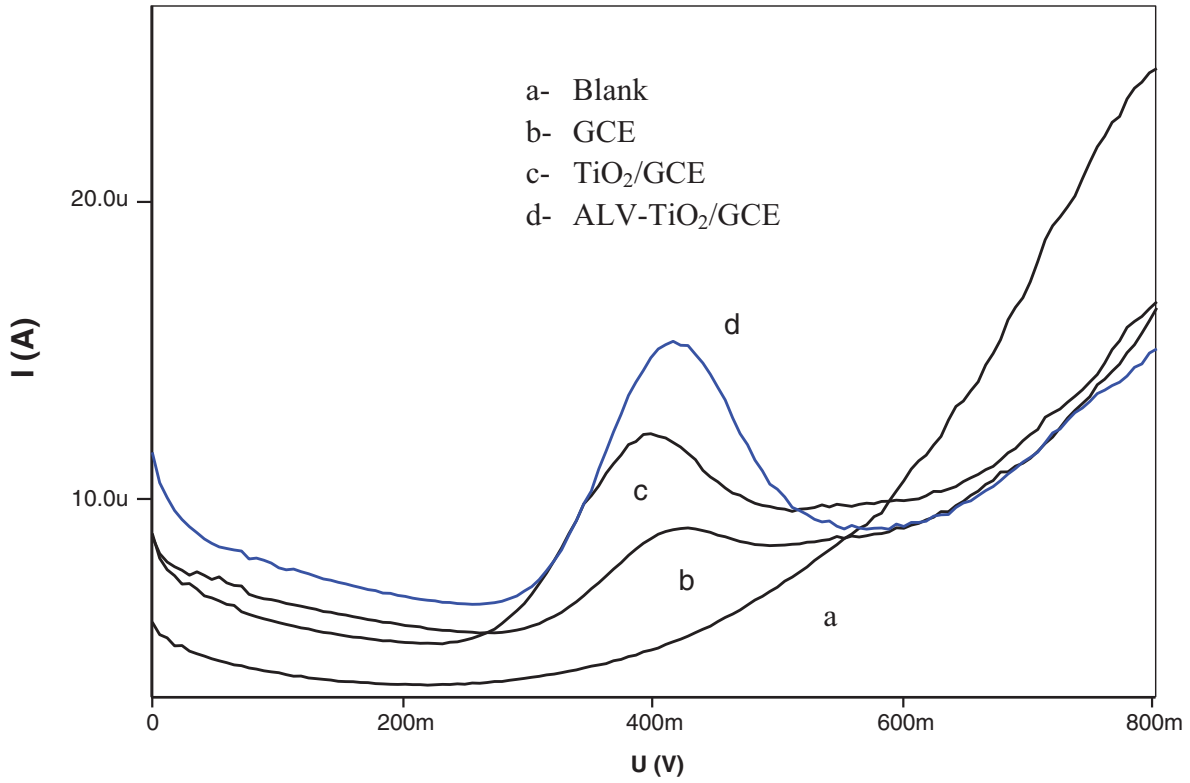

FIGURE 10 Square wave voltammograms of QRC on (a) blank, (b) bare GC, (c) TiO_2/GC, (d) ALV-TiO_2/GC sensor

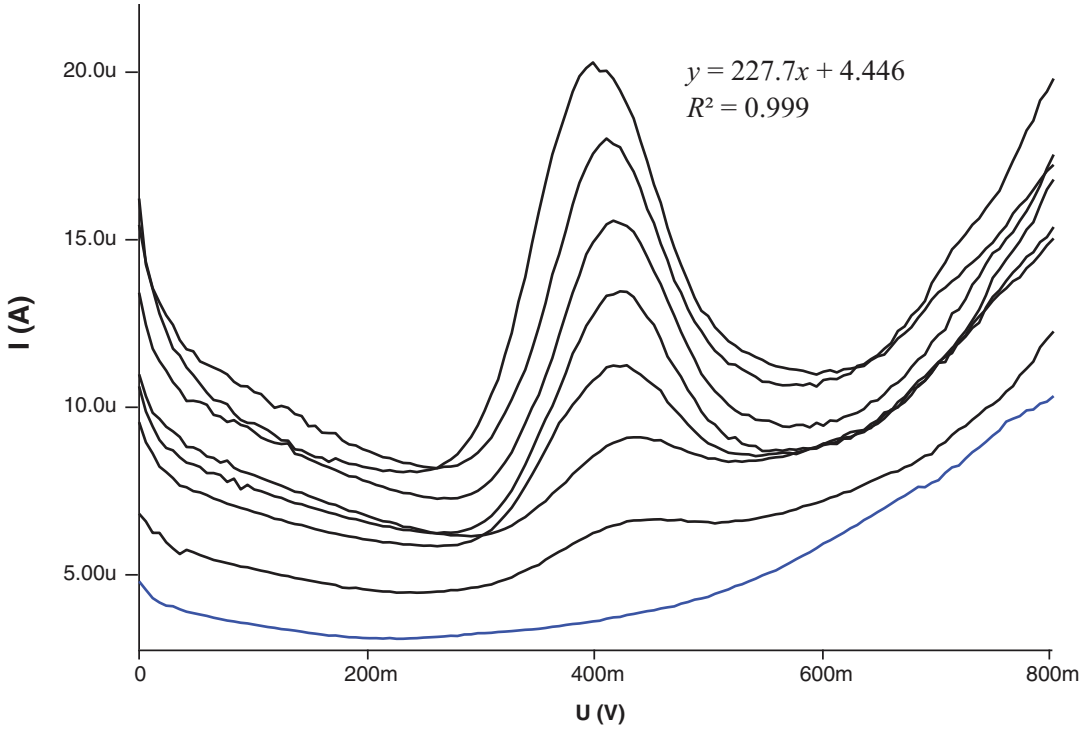

FIGURE 11 Linearity of quercetine by square wave voltammetry at GCE-*Aloe vera*-titanium oxide. Standard concentrations in BR buffer pH 3.0 are as follows: (a) blank, (b) 0.01 μg/mL, (c) 0.02 μg/mL, (d) 0.03 μg/mL, (e) 0.05 μg/mL, (f) 0.06 μg/mL, (g) 0.07 μg/mL, and (h) 0.08 μg/mL

TABLE 1 Detection limit of QRC at different electrodes

Electrode	Analytical method	Linear range	LOD	Reference
Pt-PDA@SiO2/GCE	SWV	0.05-0.383 μM	16 nM	1
Au-PAF-6/GCE	DPV	1×10^{-6} to 6×10^{-4} μM	2 nM	2
3D-rGO/CILE	CV	0.1-100 μM	65 nM	3
Fe3O4@NiO/ CPE	SWV	0.08-60 μM	2.18 nM	4
Poly(Gallic acid)/MWNT	CV	0.075-25 μM	54 nM	26
CSPE	DPV	0.016-17 μM	7.9 nM	29
ALV-TiO_2/GCE	SWV	3.3×10^{-7} to 2.31×10^{-6} μM	0.8 nM	Present study

[a]Abbreviations: platinum-polydopamine coated silica particles modified glassy carbon electrode (Pt-PDA@SiO2/GCE), Gold nanoparticles decorated on porous aromatic framework (Au-PAF-6/GCE), three-dimensional reduced graphene oxide aerogel/ carbon ionic liquid electrode (3D-rGO/CILE), magnetic nanoparticles (MNPs) modified carbon paste electrode ((Fe3O4@NiO/ CPE), Glassy carbon electrode modified with multi-walled carbon nanotubes and electropolymerized gallic acid (poly(gallic acid)/MWNT/GCE), Carbon Screen printed Electrode (CSPE).

TABLE 2 Intraday rand inter day repeatability data for QRC at ALV TiO_2/GC sensor

Intraday repeatability		
Concentration	**Average current**	**%CV**
0.04	10.27	1.46
0.05	14.17	2.82
0.07	23.17	0.99
Interday repeatability		
0.04	13.8	2.7%
0.05	19.6	2.3%
0.07	27.7	1.6%

TABLE 3 Sensor reproducibility data for QRC at ALV -TiO_2/GC sensor

Sensor reproducibility			Single sensor repeatability	
Sensor	**Mean current**	**% RSD**	**Mean current**	**% RSD**
Sensor 1	8.29[a]	0.30%	8.29[a]	0.30%
Sensor 2	8.64[a]	0.79%		
Sensor 3	8.09[a]	0.99%		
Average	8.34[b]	3.34%		

[a]Mean of three replicate reading.
[b]Mean of three sensors.

4.2 | Precision

Selectivity and sensitivity of any method are directly influenced by precision of results obtained. "Precision of method may be defined as the closeness of individual measures of an analyte, when the procedure is applied repeatedly to multiple aliquots of a single homogeneous volume of biological sample." A minimum of three concentrations in the range of expected study concentration of QRC was found to be 1.46% for 400 ng/mL, 2.82% for 500 ng/mL, and 0.99% for 700 ng/mL, which suggests that the developed method exhibits excellent precision for the quantification of quercetine.

4.3 | Reproducibility and stability of the sensor

The reproducibility of sensor was also estimated with three different electrodes that were fabricated independently by the same procedure. The RSD (Relative Standard Deviation) for peak current measuring in 0.1 M QRC demonstrates the reliability of the fabricated sensor (Table 2 & 3). Additionally, the stability of modified GCE was also investigated. For this, modified electrode was kept for a month and at the end of the month, the

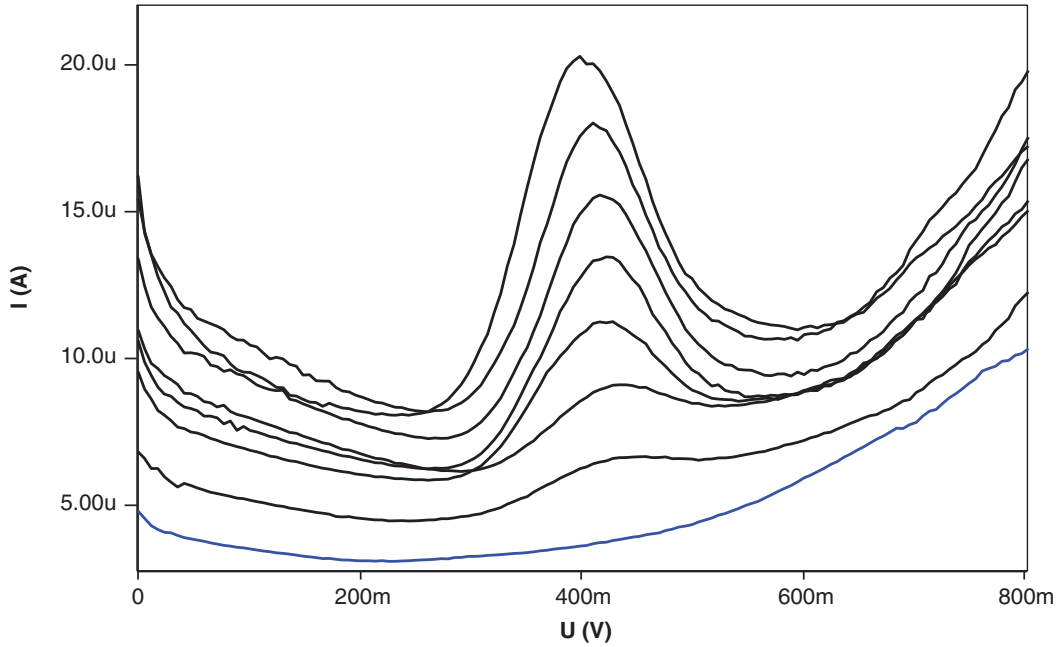

FIGURE 12 Voltammograms for different concentrations of QRC at ALV-TiO2/GC sensor in real sample

TABLE 4 Interference analysis for QRC in presence of different interferents at ALV-TiO_2/GC sensor

Interferent	Interferent concentration (μg/mL)	Recovery %
Inorganic ions (Na^+,K^+,$Ca^{2+}Cl^-$, $SO4^{2-}$, CO_3^{2-})	50	99.11%
Glucose	25	98.76%
Fructose	25	100.34%
Eugenol	25	97.78%
Capsaicin	25	99.06%
Morin	25	97.2%

peak current response was measured, which was approximately same as the original value. The excellent long-term stability and reproducibility of the prepared electrodes make them attractive as electrochemical sensors.

4.4 | Real sample analysis

In this study, real sample analysis was done by standard addition method. The procedure adopted was as follow: Seven volumetric flasks of 2.0 mL were taken and labeled as A, B, C, D, E, F, and G. To each volumetric flask, 1.0 mL of real sample was added. The flask A was diluted with ethanol up to the mark. A total of 0.01 mM standard solution of QRC was added as 0, 200, 300, 400, 500, 600 and 700 μL in labeled flask from B to G followed with dilution with ethanol up to the mark. Afterward, Voltammogrm was recorded (Figure 12) and a graph was plotted between concentration and peak response.

4.5 | Interference study

The interference analysis was performed to examine the selectivity of the sensor. The standard solution of 0.05 μg/mL QRC was prepared in ethanol. The study was observed in the presence of various interferents such as organic compounds and inorganic ions. Slight change in current of QRC was observed in the presence of above interferents (Table 4).

5 | CONCLUSION

A novel sensor is developed by modifying the GCE with a highly conductive *Aloe vera*-titanium oxide nanocomposite for the electrochemical study of the QRC by SWV (Square Wave Voltammetry) technique. Fabricated sensor exhibited tremendous sensitivity, good stability, repeatability, reproducibility, and low detection limit.

CONFLICT OF INTEREST

The authors declare no conflict of interest.

DATA AVAILABILITY

Research data are not shared.

ORCID

Antony Nitin Raja https://orcid.org/0000-0002-1915-0303

REFERENCES

1. Manokaran M, Muruganantham R, Muthukrishnaraj A, Balasubramanian N. Platinum-polydopamine @SiO2 nanocomposite modified electrode for the electrochemical determination of quercetin. *Electrochem Acta*. 2108;168:16-24.
2. Sun S, Zhang M, Li Y, He X A. Molecularly imprinted polymer with incorporated graphene oxide for electrochemical determination of quercetin. *Sensors*. 2013;13:5493-5506.
3. Niu X, Li X, Chen W, et al. Three-dimensional reduced graphene oxide aerogel modified electrode for the sensitive quercetin sensing and its application. *Mater Sci Eng C Mater Biol Appl*. 2018;89:230-236.
4. Sepideh T, Ali B. A new sensing platform based on magnetic Fe3O4@NiO core/shell nanoparticles modified carbon paste electrode for simultaneous voltammetric determination of Quercetin and Tryptophan. *J Electroanal Chem*. 2018;808:50-58.
5. Ying J, Yuan L, Binbin R, Xinsheng L, Yonghong L, Jeffrey S. Nitrogen-doped graphene-ionic liquid-glassy carbon microsphere paste electrode for ultrasensitive determination of quercetin. *Microchem J*. 2020;155:104689.
6. Zhu QG, Sujari ANA, Ghani S. Nafion-MWCNT composite modified graphite paste for the analysis of quercetinin fruits of *Acanthopanax sessiliflorus*. *Sensor Actuat B Chem*. 2013;177:103-110.
7. Muti M, Gec K, Nacak FM, Aslan A. Electrochemical polymerized 5-amino-2-mercapto-1,3,4-thiadiazole modified single use sensors for detection of quercetin. *Colloids Surf B Biointerfaces*. 2013;106:181-186.
8. Veerapandian M, Seo YT, Yun K, Lee MH. Grapheneoxide functionalized with silver@silica–polyethylene glycol hybrid nanoparticles for direct electrochemical detection of quercetin. *Biosens Bioelectron*. 2014;58:200-204.
9. Rembiesa J, Garia H, Engbloma J, Ruzgas T. Amperometric monitoring of quercetin permeation through skin membranes. *Int J Pharm*. 2015;496:636-643.
10. Zielinska D, Nagelsb L, Piskuła MK. Determination of quercetin and its glucosides in onion by electrochemical methods. *Anal Chim Acta*. 2008;617:22-31.
11. Tokuşoğlu O, Ünal MK, Yıldırım Z. HPLC–UV and GC–MS characterization of the flavonol aglycons quercetin, kaempferol, and myricetin in tomato pastes and other tomato-based products. *Acta chromatogr*. 2003;13:196-207.
12. Casagrand R, Baracat MM, Georgetti SR, et al. Method validation and stability study of quercetin in topical emulsions. *Quim Nova*. 2009;37:1939-1942.
13. Yue-ling M, Yu-jie C, Ding-rong W, Ping C, Ran X. HPLC determination of quercetin in three plant drugs from genus sedum and conjecture of the best harvest time. *Pharmacogn J*. 2017;9:725-728.
14. Sri KV, Ratna JV, Annapurna A, Kumar R. Reversed-phase HPLC method for determination of quercetin in human plasma. *Asian J Chem*. 2009;21:101-104.
15. Sengupta B, Sengupta PK. The interaction of quercetin with human serum albumin: a fluorescence spectroscopic study. *Biochem Biophys Res Commun*. 2009;299:400-403.
16. Ravichandran R, Rajendran M, Devapiriam D. Antioxidant study of quercetin and their metal complex and determination of stability constant by spectrophotometry method. *Food Chem*. 2014;146:472-478.
17. Dias FDS, Silva MF, David JM. Determination of quercetin, gallic acid, resveratrol, catechin and malvidin in Brazilian wines elaborated in the Vale do São Francisco using liquid–liquid extraction assisted by ultrasound and GC-MS. *Food Anal Methods*. 2013;6:963-968.
18. Watson DG, Oliveira EJ. Solid-phase extraction and gas chromatography–mass spectrometry determination of kaempferol and quercetin in human urine afterconsumption of Ginkgo biloba tablets. *J Chromatogr B*. 1999;723:203-210.
19. Gupta VK, Golestani F, Ahmadzadeh S, Maleh HK, Fazli G, Khosravi S. NiO/CNTs nanocomposite modified ionic liquid carbon paste electrode as a voltammetric sensor for determination of quercetin. *Int J Electrochem Sci*. 2015;10:3657-3667.
20. Wang MY, Zhang D, Tong Z, Xu X, Yang X. Voltammetric behavior and the determination of quercetin at a flowerlike Co3O4 nanoparticles modified glassy carbon electrode. *J Appl Electrochem*. 2011;41:189-196.
21. Jose F, Gomez V, Espino M, Fernandez MA, Raba J, Silva MF. Enhanced electrochemical detection of quercetin by natural deep eutectic solvents. *Anal Chim Acta*. 2016;936:91-96.
22. Vu DL, Žabčíková S, Červenka L, Ertek B, Dilgin Y. Sensitive voltammetric determination of natural flavonoid quercetin on a disposable graphite lead. *Food Technol Biotechnol*. 2015;53:379-384.
23. Zhang Z, Gu S, Ding Y, Shen M, Jiang L. Mild and novel electrochemical preparation of β-cyclodextrin grapheme nanocomposite film for super-sensitive sensing of quercetin. *Biosens Bioelectron*. 2014;57:239-244.

24. ElÅin S, Yola ML, Eren T, Girgin B, Atar N. Highly selective and sensitive voltammetric sensor based on ruthenium nanoparticle anchored calix[4]amidocrown-5 functionalized reduced graphene oxide: simultaneous determination of quercetin, morin and rutin in grape wine. *Electroanalysis*. 2016;28:611-619.
25. Şenocak A, Köksoy B, Demirbaş E, Basova T, Durmuş M. 3D SWCNTs-coumarin hybrid material for ultra-sensitive determination of quercetin antioxidant capacity. *Sensor Actuat B Chem*. 2018;267:165-173.
26. Guzel Z, Ekaterina K, Herman B. Poly(gallic acid)/MWNT-modified electrode for the selective and sensitive voltammetric determination of quercetin in medicinal herbs. *J Electoanal Chem*. 2018;821:73-81.
27. Karthika A, Ramasamy VR, Karuppasamy P, Suganthi A, Rajarajan M. A novel electrochemical sensor for determination of hydroquinone in water using FeWO4/SnO2 nanocomposite immobilized modified glassy carbon electrode. *Arab J Chem*. 2020;13:4065-4081.
28. Annamalai K, Ayyadurai S, Muthuramalingam R. An in-situ synthesis of novel V2O5/G-C3N4/PVA nanocomposite for enhanced electrocatalytic activity toward sensitive and selective sensing of folic acid in natural samples. *Arab J Chem*. 2020;13:3639-3652.
29. Karthika A, Rosaline DR, Inbanathan SSR, Suganthi A, Rajarajan M. Fabrication of cupric oxide decorated β-cyclodextrin nanocomposite solubilized Nafion as a high performance electrochemical sensor for L-tyrosine detection. *J Phy Chem Solids*. 2020;136:109145.
30. Yao YY, Zhang L, Wang Z, Xu J, Wen Y. Electrochemical determination of quercetin by self-assembled platinum nanoparticles/poly(hydroxymethylated-3,4- ethylenedioxylthiophene) nanocomposite modified glassy carbon electrode. *Chin Chem Lett*. 2014;25:505-510.
31. Donga CD, Chena CW, Kao CM, Hung CM. Synthesis, characterization, and application of CuO-modified TiO_2 electrode exemplified for ammonia electro-oxidation. *Process Saf Environ Prot*. 2017;112:243-253.
32. Shettia PN, Nayaka DS, Malodea SJ, Kulkarni RM. An electrochemical sensor for clozapine at ruthenium doped TiO_2 nanoparticles modified electrode. *Senor Actuat B Chem*. 2017;247:858-867.
33. Tsele TP, Adekunle AS, Fayemi OE, Ebenso EE. Electrochemical detection of epinephrine using polyaniline nanocomposite films doped with TiO_2 and RuO_2 nanoparticles on multi-walled carbon nanotube. *Electrochim Acta*. 2017;243:331-348.
34. Liao J, Yang F, Wang C, Lin S. The crystal facet-dependent electrochemical performance of TiO_2 nanocrystals for heavy metal detection: theoretical prediction and experimental proof. *Sensor Actuat B Chem*. 2018;271:195-202.
35. Tian X, Liu L, Li Y, et al. Nonenzymatic electrochemical sensor based on CuO-TiO_2 for sensitive and selective detection of methyl parathion pesticide in ground water. *Sensor Actuat B Chem*. 2018;256:135-142.
36. Prasad MS, Chen R, Ni H, Kumar KK. Directly grown of 3D-Nickel oxide nano flowers on TiO_2 nanowire arrays by hydrothermal route for electrochemical determination of naringenin flavonoid in vegetable samples. *Arab J Chem*. 2020;13:1520.
37. Mavric T, Bercina M, Imani R, et al. Electrochemical biosensor based on TiO_2 nanomaterials for cancer diagnostics. In: A.Iglič, M.Rappolt, A. J.García-Sáez, eds. *Advances in Biomembranes and Lipid Self Assembly*. Vol. 27. Cambridge, MA: Academic Press; 2018:63-105.

How to cite this article: Raja AN, Pandey A, Jain R. Development of *Aloe vera*-titanium oxide-based ultrasensitive sensor for the quantification of quercetin. *Anal Sci Adv*. 2020;1:56–69. https://doi.org/10.1002/ansa.202000010